Chapter 8

U-Pb Detrital Zircon Geochronology of Iron Ore Conglomerates of the Chamakpur Member: Implications for the Origin of High-grade Iron Ore

8.1. Introduction

The high-grade iron ore deposits with >60 wt % of Fe are essentially mined from BIF-host rocks of Archeran greenstone belts and Proterozoic platformal sequences. The origin and timing of ore genesis for these BIF-hosted high grade deposits remain as one of the most investigated research area during the past couple of decades particularly with the sharp increase in demand for the iron and steel industry (*for reviews* Hagemann et al. 2008, 2016). The BIF hosted iron ore deposits are interpreted in terms of three genetic processes, e.g., hydrothermal, supergene and supergene-modified hydrothermal processes (Beukes et al. 2003). World's largest iron ore resources are mainly located in Australia, Brazil, China, India, Russia, South Africa, West Africa, Ukraine and United States (USGS 2017) (Fig. 8.1). The deposits are mainly hosted by Paleo-Neoarchean greenstone belts such as Singhbhum-Odisha Dharwar and Bastar cratons in India (Mukhopadhyay et al. 2008a, 2008b; Mukhopadhyay et al. 2012), Hamersley Group (~2.5 Ga), Pilabara craton Western Australia (Morris 1985; Harmsworth et al. 1990), Paleoproterozoic Cauê Formation, Itabira Group in the Quadrilátero Ferrífero Minas Gerais (~2.6 Ga) or slightly older Carajás Formation (~2.8 Ga) in Brazil (Spier et al. 2008; Klein and Laderia 2000; Rosière and Rios 2004), Sishen-Beeshoek and Thabazimbi deposits of Paleoproterozoic Kuruman and Penge iron formations in the Transvaal-Griquatown belts of South Africa (Beukes et al. 2003), Kursk iron ore deposits in Russia and Kola

peninsula iron ore deposits in Ukraine from Paleoproterozoic age (Belykh et al. 2007; Bekker et al. 2010) and BIF hosted iron formation of Neoarchean- Proterozoic successions of the Keewatin and Animikee Groups in the Lake District of United States and Canada (~2.7-1.9 Ga). The iron ore formation is essntially a process of enrichment of iron at the expense of silica in the host BIF. The ore genetic process and subsequent modifications exert primary controls on the ore mineralogy and ore texture and commonly involve multiple phases.

Although the depositional ages and stratigraphic status of host BIF successions for most of these deposits are unequivocally established, the timing of ore formation for most of these deposits remain yet to be constrained primarily because of lack of datable mineral constituent related to ore genesis and subsequent alteration processes (Table 8.1). Indirect geological evidences such as occurrence of ancient detrital ores in the younger succession as well as cross-cutting igneous intrusions are the only clues to constraint the relative age of ore formation in some of the deposits. For examples the ca. 2008 Ma constraints the ore genesis of the Hammerserly basin to ca. 2050–2000 Ma (Müller et al. 2005). Similar examples from ore pebble conglomerates at the base of Gamagara/Mapedi red bed succession of the Keis (formerly Kheis) Supergroup overlying Sishen and Beeshoek deposits brackets the ore genesis episodes between 2.22 Ga to 2.06 Ga (*review in* Smith and Beukes 2016).

The timing of ore formation is also not well coinstrained for the BIF-hosted high grade iron ore deposits of India. Mukhopadhyay et al. (2007) documented lenticular bodies of the pebbly iron ore conglomerate from the Chamakpur mines within the present study area (Fig. 8.2). Based on stratigraphic consideration a Neoarchean to

Fig. 8.1. Major Iron Ore Deposits of the world showing age of the host BIF succession (marked in blue ink within bracket) and available age data of ore formation (marked in green ink) from some of the deposits. Labrador Trough (Conliffe 2015)[1]; Animikie group (Goodwin 1996, p. 140)[2]; Carajás Formation (Figueiredo e Silva et al. 2011)[3]; Cauê Formation, Itabira Group Quadrilátero Ferrífero (Cabral et al. 2012)[4]; Urucum (Beukes et al. 2003)[5]; Sishen-Beeshoek (Smith and Beukes 2016)[6]; Thabazimbi deposits (Smith and Beukes 2016)[7]; Mt. Nimba (Force 1983)[8]; Krivoy Rog (Sośnicka et al. 2015)[9]; Bailadila (Muklhopadhyay et al. 2008a)[10]; Goa (Mukhopadhyay et al. 2008a)[11] ; Donimalai (Mukhopadhyay et al. 2008a)[12]; Noamundi (Mukhopadhyay et al. 2008a)[13]; Hamersley Group, Western Australia (Morris 1985;Harmsworth et al. 1990)[14].

Paleoproterozoic age of the conglomerates was suggested by Mukhopadhyay et al. (2007). However, there is no geochronolgic constraint on the depositional age of the conglomerate body. The depositional age constraints on these iron ore clast-bearing conglomerates would in turn throw light on the minimum age of the primary orebody from which such clasts were sourced and in turn would bear implications for the origin of the deposit at the source. In the present work I have attempted to constraint the age of deposition of the conglomerates from detrital zircon U-Pb ages of the sandstone clasts that are associated with iron ore clasts from same conglomerate bodies.

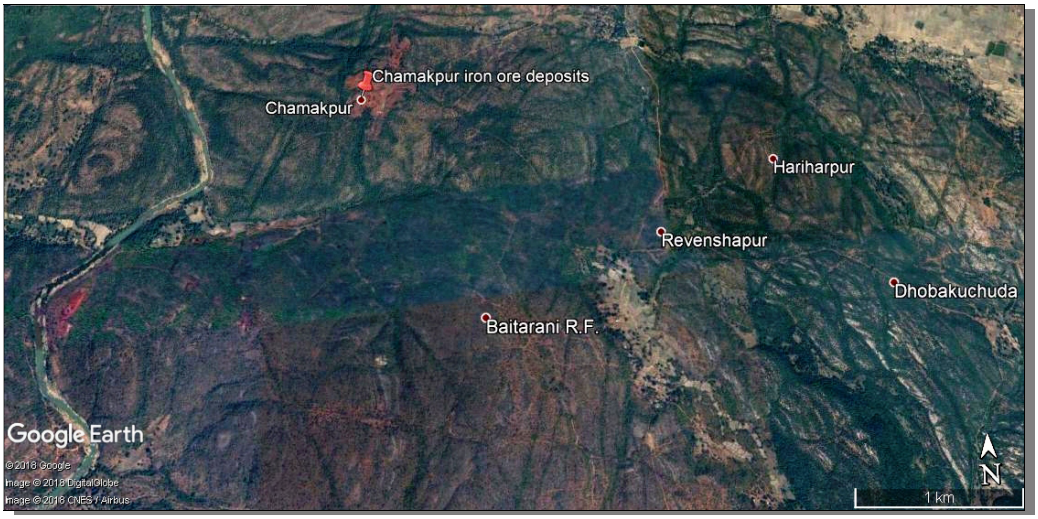

Fig. 8.2. Google map for location of the Chamakpur iron ore deposit.

8.2. Methodology

8.2.1. Petrographic analysis

Fresh iron ore conglomerate samples were collected from the Chamakpur area covering the range of the stratigraphy. About 15 Polished thin-sections were prepared for petrographic and SEM-EDS studies. The petrographic study was carried out with a Nikon POl200 petrological microscope at Presidency University, Kolkata. Carbon-coated thin sections were carried out by a TESCAN VEGA-LSU scanning electron microscope (SEM) at the Presidency University, Kolkata. This instrument was

commonly operated at 30 kV and a beam current of 10 nA. Back Scattering Electron (BSE) and Secondary Electron (SE) images were recorded in 22-25 mm working distance.

8.2.2. Laser ablation SF-ICP-MS U-Pb dating (Federal University of Ouro Preto, UFOP)

Total 79 detrital zircon grains from Keonjhar Quartzite were analyzed at Federal University of Ouro Preto. This analysis were carried out by using a Thermo-Finnigan Element 2 sector field ICP-MS coupled to a CETAC213 ultraviolet laser system, at UFOP (Gerdes and Zeh 2006; Moreira *et al.* 2016, Farina et al. 2015 Schoene et 2006). Laser ablation is commonly operated spot size of 20 μm, ablation spot depth 15-20 μm. Data were acquired in peak jumping mode during 20s background measurement followed by 20s sample ablation. The signal was tuned for maximum sensitivity for Pb and U while keeping oxide production well below 1%. Raw data were corrected for background signal, common Pb, laser-induced elemental fractionation, instrumental mass discrimination, and time-dependent elemental fractionation of Pb/U using an in-house MS Excel spreadsheet program (e.g., Gonçalves *et al.* 2016). The common Pb correction was based on the Pb composition model (Stacey and Kramers 1975). Laser-induced elemental fractionation and instrumental mass discrimination were corrected by normalization to the reference zircon GJ-1 (Jackson *et al.* 2004), which was analyzed during the analytical session under exactly the same conditions as the samples. Prior to this normalization, the drift in elemental fractionation was corrected by applying a linear regression through all measured ratios, excluding the outliers (N ± 2SD), and using the intercept with the y-axis as the initial ratio. The total offset of the measured drift-corrected $^{206}Pb/^{238}U$ ratio

from the "true" ID-TIMS value of the analyzed GJ-1 grain was typically around 1 - 3%. Reported uncertainties (2σ) were propagated by quadratic addition of the external reproducibility (2SD) obtained from the zircon reference material GJ-1 during the individual analytical session.

At UFOP, three secondary standards were used before and during runs: Plešovice zircon (337 ± 1 Ma; Sláma *et al.* 2008), M127 zircon (524 ± 1 Ma; Klötzli *et al.* 2009) and 91500 zircon (1065.4 ±0.6 Ma; Wiedenbeck *et al.* 1995). The results are within error of recommended TIMS ages. Sixty-two analyses of Plešovice zircon gave a Concordia age of 338.39 ± 0.72 Ma (mean $^{206}Pb/^{238}U$ age = 338 ± 1; mean $^{207}Pb/^{235}U$ age = 338 ± 1Ma). Thirty-four analyses of M127 zircon gave a Concordia age of 526 ± 1 Ma (mean $^{206}Pb/^{238}U$ age = 526 ± 1; mean $^{207}Pb/^{235}U$ age = 525 ± 1.2 Ma). Twenty-three analyses of 91500 zircon gave a Concordia age of 1060 ± 3.4 Ma (mean $^{206}Pb/^{238}U$ age = 1059 ± 4.2; mean $^{207}Pb/^{235}U$ age = 1061 ± 3.7 Ma).

8.3. Description

8.3.1. Mode of occurrence of the iron ore conglomerates

The iron ore conglomerate body in the Keonjhar Quartzite occurs in the upper part of the succession (Fig. 8.3A). The iron ore clast-bearing conglomerates occur as amalgamated lensoid mass-flow deposits incised within mature shallow shelf succession (Fig. 8.3B). The clast size varies among lenses and range from cobble/boulder size to pebble size. Clasts include hard hematitic iron ore, BIF and sandstones. The ore conglomerate bearing interval is about 40 m thick and represents ~220 m along strike incised valley fill deposit within shelf environment.

A.

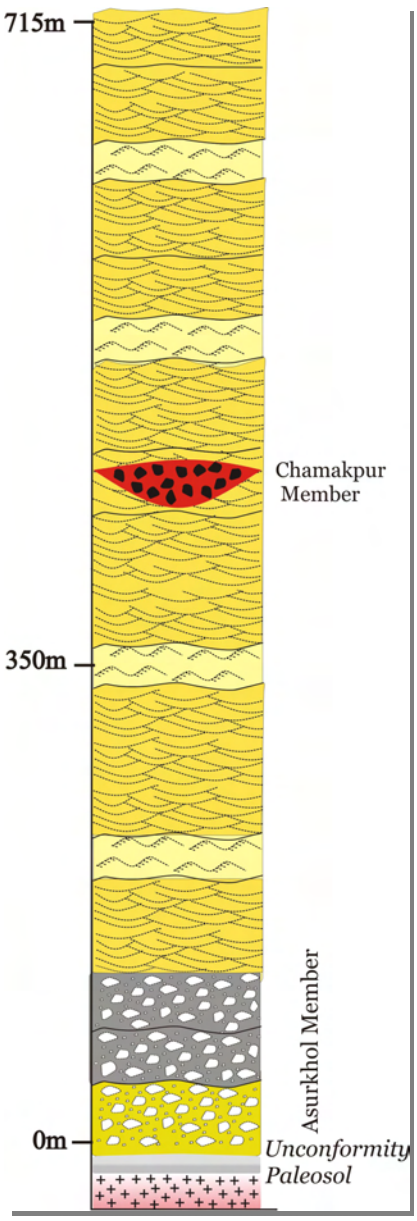

B.

C.

Fig. 8.3. A. Composite stratigraphic succession of the Keonjhar Quartzite. Note: two members classified within this formation: Asurkhol Member and Chamakpur Member. The Chamakpur Member occurs as lentil and is entirely represented by iron ore clast-bearing conglomerates. B. Field photograph of lensoid iron ore conglomerate bodies mined out from Chamakpur Member. C. Field photograph of iron ore conglomerate with clasts of hard iron ore (dark steel gray) and BIF (reddish) in Chamakpur Member.

This lensoid iron ore conglomerate body is overlain by ~215 m thick mature trough cross-stratified sandstone. The iron ore clasts are so predominant component in these conglomerates that the conglomerates are mined as low-grade (~55 wt % to 45 wt % Fe) iron ores. The conglomerates are very unique in a sense that they are encased in a

shelf sandstone host succession and the ore clasts are remarkably similar with the hard laminated or hard massive ores of the neighbouring BIF-hosted high-grade deposits of the Noamundi-Joda iron ore district (Fig. 8.3C).

8.3.2. Iron ore petrography

The predominant ore minerals in iron oxides bands are idiotopic (equant), anhedral, microplaty and microcrystalline hematite/martite (Fig. 8.4, 8.5). The different

A.

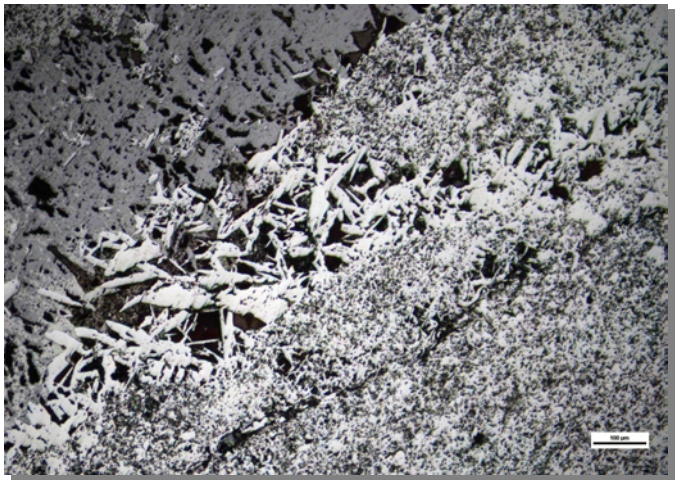

B.

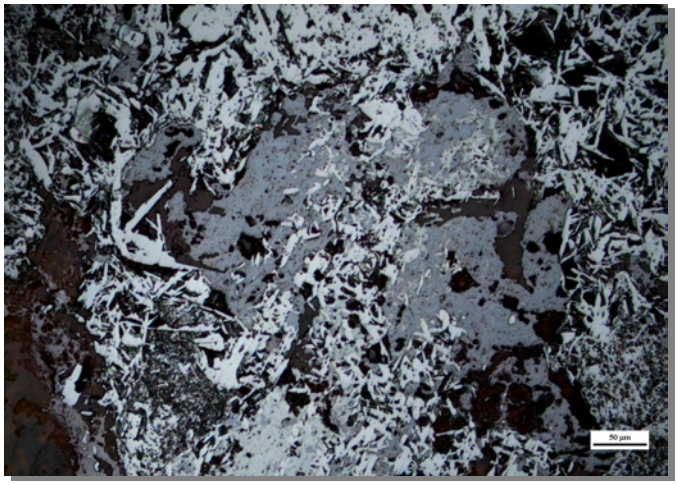

Fig. 8.4. Reflected light photomicrograph of A. specularite blades associated with anhedral and microplaty hematite. B. Quartz grain (dark gray) surrounded by anhedral and microplaty hematite.

morphological forms of hematite define mosaic texture with varying porosity in hard/laminated ores from the ore clasts of the conglomerate. The iron ore conglomerate is partly oxidized and are composed of anhedral to microcrystalline

hematite and martite. The matrix of the iron conglomerate is mainly crypto- to-microcrystalline hematite and detrital quartz sand.

8.4. Detrital zircon U-Pb geochronology

The U-Pb data for 79 detrital zircons (mainly magmatic nature with oscillatory zoning) are summarized in (Table 6.1; details in chapter 6). The zircons represent samples from the sandstone clasts of iron ore-bearing conglomerate (INIC 1, with Th/U in range of 0.09 to 0.91) and from sandstone horizons about 60 m above the iron ore conglomerate horizons within the Keonjhar Quartzite. The INIC 2 (Th/U ratio within range of 0.03 to 0.47) samples from the stratigraphy well above the conglomerates have been analysed to widen the stratigraphic range for constraining the maximum age of deposition of the host succession. It may be mentioned here that detrital zircon age from U-Pb systematics have been reported from the basal part of the Keonjhar Quartzite by Mukhopadhyay et al. (2014). Therefore, the detrital zircon U-Pb ages from three widely separated stratigraphic intervals within the ~715 m thick Keonjhar Quartzite succession are reasonably well constrained for maximum depositional age of the succession.

The histogram of U-Pb age distribution from two samples analyzed here reveal two major peaks at 3.1 and 3.2 Ga (Fig. 8.6). The minimum age population is represented by INIC 2 with a small peak at 3000.39 Ma. The minimum depositional age population of these zircons are shown in a histogram is around 3041.57 Ma (Table 6.1, details in chapter 6).

The zircons from sandstone clast and upper horizons of sandstone show depositional age ranges from 3000–3256 Ma (those zircons with <5% discordance limit have been considered). The detrital zircon U-Pb age data, therefore,

A.

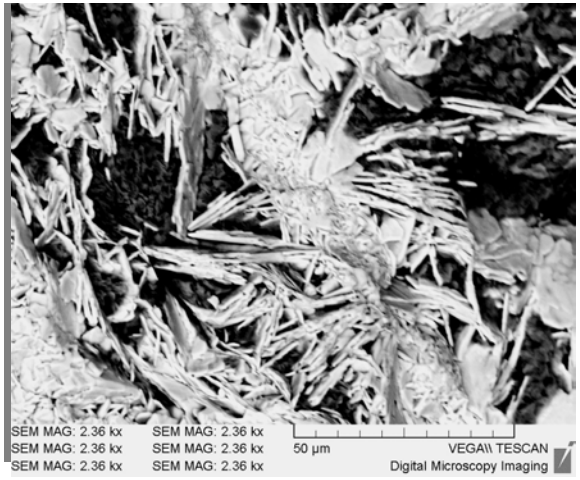

B.

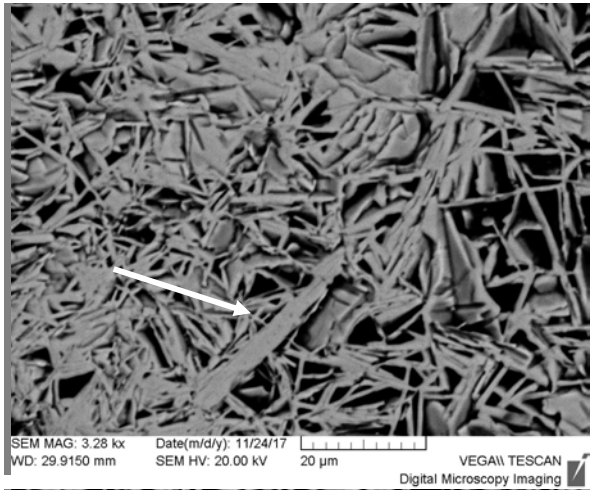

C.

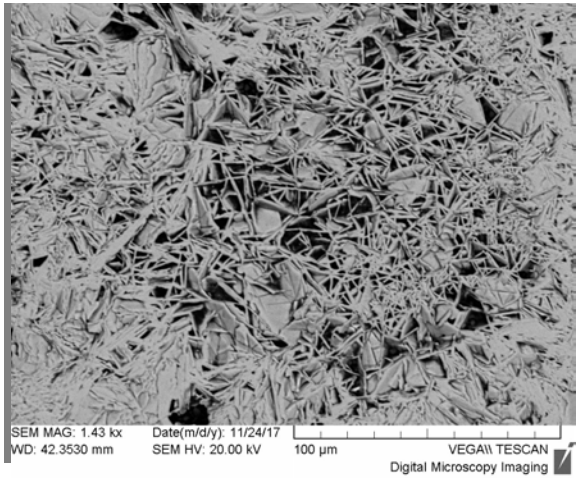

D.

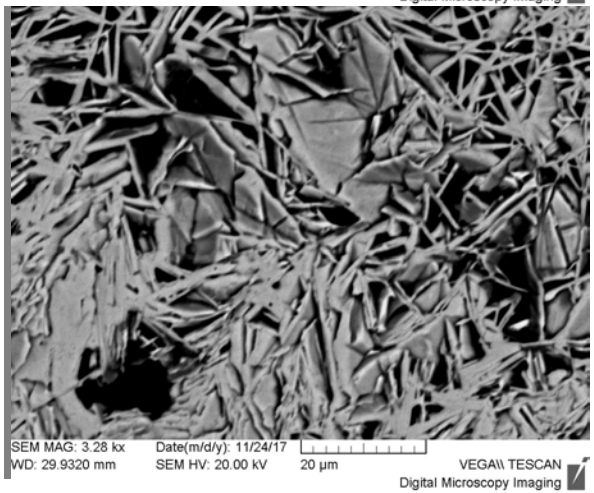

Fig. 8.5. BSE-SEM images of A. Idiotopic hematite (martite) surrounded by microplaty hematite. B. Specularite blades (arrow) in network of microplaty hematite. C. Anhedral and microplaty hematite forming mosaic texture for hard ores in ore pebble. D. Anhedral and microplaty hematite network revealing porosity distribution in hard ores from iron ore pebble in conglomerate.

suggest that the primary hard iron ore formation age at source deposits from where the clasts were derived is at least older than 3000.39 Ma.

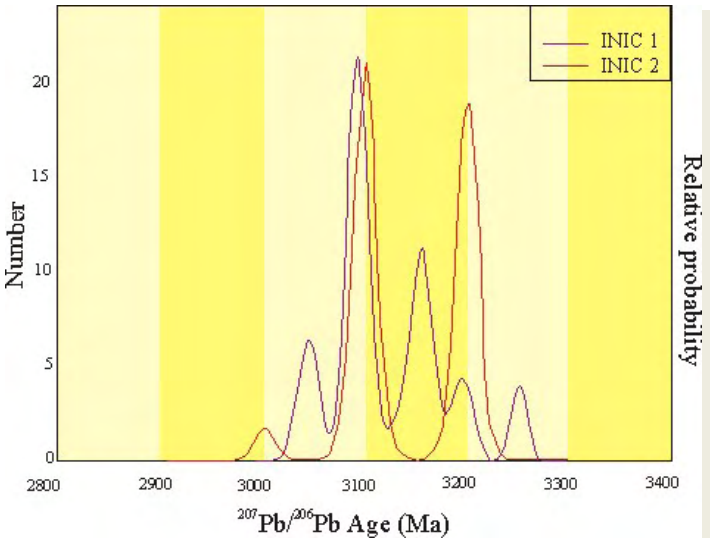

Fig. 8.6. Detrital zircons LA-ICPMS U-Pb age ranging from 3000–3256 Ma (considered those zircons with <5% discordance limit) from sandstone clasts in iron ore conglomerate and overlying sandstone beds of Keonjhar Quartzite.

8.5. Discussion

8.5.1. Controls on iron ore conglomerate deposition

The deposition of this type of iron ore conglomerate within thick shelf sandstone is in fact difficult to explain. The conglomerate in shelf sandstone marks a major base level fall and fluvial incision on the wave-agitated shelf. The fluvial incision in shelf implies a condition of forced regression. Forced regression on the other hand is a result of combining effect of eustatic fall and tectonic uplift (Catuneanu 2006). In case of the Chamakpur iron ore conglomerates the base level fall in the upper part of the Keonjhar Quartzite succession may be due to such eustatic and tectonic factors.

8.5.2. Implication for the age of primary ore

The detrital zircon ages from the sandstone clast of the iron ore conglomerate suggest that iron ore mineralization in the source of these conglomerates predated the depositional age of the host Keonjhar Quartzite succession and fixes the lower limit of the ore formation at around 3 Ga. The minimum depositional age of the upper

sandstone body is around 3 Ga and represents the oldest iron ore deposit of the world so far investigated (Table 8.1, Fig. 8.6). The age constraints further suggests implications for BIF enrichment process by oxide phase Fe-minerals (hematite/magnetite) during an oxygen-deficient/reducing stage of Mesoarchean atmosphere (Lyons et al. 2014)

Table 8.1. Major Iron Ore Deposits of the World showing age of the host BIF succession and available age data of ore formation from some of the deposits.

Iron Formations		Depositional age of host succession	Age of iron ore formation
Ukrainian Shield	Krivoy Rog (Sośnicka et al. 2015)	2.2 Ga	No data
North American Platform (Lake Superior District)	Labrador Trough (Conliffe 2015)	2.17 Ga to 2.87 Ga	2.17 Ga to 1.79 Ga (New Quebec orogeny)
	Animikie group (Goodwin 1996)	1.85 Ga to 2.1 Ga	No data
Brazilian Shield (Amazonia-Sao Farncisco craton)	Cauê Formation, Itabira Group Quadrilátero Ferrífero (Cabral et al. 2012)	2.65 Ga	No data
	Carajás Formation (Figueiredo e Silva et al. 2011)	2.7 Ga to 2.8 Ga	1.717 Ga
	Urucum (Beukes et al. 2003)	~700 Ma	<700 Ma
Australian Shield	Hamersley Group, Western Australia (Morris 1985; Harmsworth et al. 1990)	~2.5Ga	~2.2 Ga
Indian Shield	Noamundi (Mukhopadhyay et al. 2008a and 2008b)	3.4 Ga	No data
	Bailadila (Mukhopadhyay et al. 2008a)	2.7 to 2.45	No data
	Goa (Mukhopadhyay et al. 2008a, 2008b)	2.7 Ga	No data
	Donimalai (Mukhopadhyay et al. 2008a, 2008b)	2.7 Ga	No data
Kaapvaal Craton (South Africa)	Sishen-Beeshoek (Smith and Beukes 2016)	2.6 to 2.2 Ga	2.22 to 2.06 Ga
	Thabazimbi deposits (Smith and Beukes 2016)		1.93 Ga to 2.047 Ga
Liberian Shield	Mt. Nimba (Force 1983)	2.7 Ga	No data